



UNIVERSITY OF LEEDS

This is a repository copy of *Pyrolysis-catalytic steam/dry reforming of processed municipal solid waste for control of syngas H₂:CO ratio*.

White Rose Research Online URL for this paper:

<https://eprints.whiterose.ac.uk/197152/>

Version: Accepted Version

Article:

Penney, TK, Nahil, MA and Williams, PT orcid.org/0000-0003-0401-9326 (2022) Pyrolysis-catalytic steam/dry reforming of processed municipal solid waste for control of syngas H₂:CO ratio. *Journal of the Energy Institute*, 102. pp. 128-142. ISSN 1743-9671

<https://doi.org/10.1016/j.joei.2022.03.001>

© 2022 Energy Institute. This manuscript version is made available under the CC-BY-NC-ND 4.0 license <http://creativecommons.org/licenses/by-nc-nd/4.0/>.

Reuse

This article is distributed under the terms of the Creative Commons Attribution-NonCommercial-NoDerivs (CC BY-NC-ND) licence. This licence only allows you to download this work and share it with others as long as you credit the authors, but you can't change the article in any way or use it commercially. More information and the full terms of the licence here: <https://creativecommons.org/licenses/>

Takedown

If you consider content in White Rose Research Online to be in breach of UK law, please notify us by emailing eprints@whiterose.ac.uk including the URL of the record and the reason for the withdrawal request.



eprints@whiterose.ac.uk
<https://eprints.whiterose.ac.uk/>

Pyrolysis-catalytic steam/dry reforming of processed municipal solid waste for control of syngas H₂:CO ratio

Thomas K. Penney, Mohamad A. Nahil, Paul T. Williams*

School of Chemical and Process Engineering, University of Leeds, Leeds, LS2 9JT, U.K.

(*Corresponding author; Email; p.t.williams@leeds.ac.uk; Tel; #44 1133432504)

Abstract

The production of syngas from the pyrolysis-catalytic reforming of processed municipal solid waste in the form of refuse derived fuel has been investigated experimentally using a two-stage fixed bed reactor with a 10 wt.% Ni-Al₂O₃ catalyst. The reforming gases used were a combination of steam and carbon dioxide (dry reforming). The main focus of the research was to manipulate the H₂:CO ratio in the syngas for targeted end-use applications by optimising the process conditions, including the input steam/CO₂ reforming gas ratio. The experimental results showed that at higher steam:CO₂ ratios, there was a marked increase in H₂ yield due to the endothermic nature of the steam and CO₂ reforming processes. The catalytic reforming temperature also had a major influence on H₂ yield, with increasing temperature raising the hydrogen yield to a maximum of ~41.0 mmol g_{RDF}⁻¹ at 955°C catalyst temperature. The H₂:CO molar ratio was also affected by the process variables and were interdependent on them. For example, the influence of an increase in the catalytic reforming temperature as the content of steam in the reforming gas input was also increased, produced a maximum H₂:CO molar ratio of ~4.7:1 achieved at an input steam:CO₂ ratio of 75:25 and a catalyst temperature of 700 °C. Whereas, at higher CO₂ content in the reforming gas, the product H₂:CO ratio was ~1:1. Also, for a steam:CO₂ input ratio of 50:50, the H₂:CO ratio produced was ~2:1 and for higher steam content in the reforming gas the product H₂:CO was ~3:1. Design of Experiments (DoE) modelling was carried out using the experimental data to identify the process conditions that would produce a target syngas H₂:CO molar ratio of 1:1 and 2:1. The predicted optimised process conditions from the DoE modelling produced experimental results close to the targeted syngas H₂:CO molar ratios, thereby validating the DoE model.

Keywords: Municipal solid waste; Refuse derived fuel; Pyrolysis; Catalysis; Syngas; Design of Experiments

1. INTRODUCTION

Biomass is viewed as an alternative carbon neutral fuel compared to fossil fuels and has the potential to realise a decarbonised and sustainable future energy supply. Second generation biomass based on derived waste sources, include, municipal solid waste, commercial waste, agricultural and animal wastes [1]. More than 220 million tonnes of municipal solid waste (MSW) is generated in Europe each year and almost 300 million tonnes of MSW is produced in the US [2,3]. Such enormous tonnages of MSW represents a substantial source of waste lignocellulosic biomass and a major feedstock for the production of biofuels. However, MSW is a difficult waste to process for the production of biofuels since it is variable in composition, contains bulky waste items and has a high moisture and ash content. However, an abundant supply of processed MSW is available in the form of Refuse Derived Fuel (RDF) and Solid Recovered Fuel (SRF). RDF and SRF produced from MSW are more compositionally homogeneous, of consistent size, with low ash and moisture content. SRF in the EU is a regulated and defined waste derived fuel complying with specified composition under European Standard EN 15359. RDF is a waste derived fuel but with no official definition, therefore, content and quality may vary. A typical system for the production of SRF/RDF consists of: sorting or mechanical separation, size reduction (shredding, chipping, milling), separation and screening, blending, drying and pelletising, packing and storage [4]. SRF/RDF may be produced from a range of different single or mixed waste streams including not only MSW, but also commercial waste, industrial waste and construction and demolition wastes [5]. The composition and properties of SRF/RDF will vary according to the origin of waste material and the sorting/separation process. SRF/RDF produced from MSW is largely composed of biomass (paper, card, wood) and waste plastics (mainly polypropylene, polyethylene, polyethylene terephthalate and polystyrene) and is produced through the removal of the metals, glass, food waste and fines from the MSW. The content of biomass material in SRF/RDF derived from MSW can range from 11 - 82 wt.% and the plastic content can range from 13- 45 wt.% depending on the input waste source and waste processing system [6].

The use of alternative feedstock sources such as biomass and wastes for the production of synthesis gas (syngas) composed of mainly hydrogen and carbon monoxide is a current high interest research topic [7-15]. Production of a high calorific value, H₂/CO-rich syngas from SRF/RDF is therefore of interest as a potentially viable option for a more

sustainable management of municipal solid waste. The hydrogen to carbon monoxide ratio of syngas is an important property, since, depending on the potential end-use application of the syngas an optimum ratio is required. For example, Song and Guo [16] and Rauch et al. [8] have described the range of syntheses possible using syngas to produce; liquid fuels through Fischer Tropsch synthesis, high value chemicals (e.g. aldehydes and alcohols) through the hydroformylation reaction and the production of methanol through catalytic reaction with syngas. The properties of the syngas, in particular the H₂:CO molar ratio influence the potential end-use synthesis of the syngas, for example an ideal H₂:CO molar ratio for Fischer Tropsch (FT) synthesis for liquid fuels production is reported to be between 1.7:1 and 2.2:1 [8, 17-19]. The production of aldehydes via the hydroformylation process requires a H₂:CO ratio of 1:1 [16, 20]. A H₂:CO ratio between 1.5:1 - 2:1 can be used for the production of methanol [8, 16, 21] and for the synthesis of dimethyl-ether an optimum H₂:CO molar ratio of 1:1 has been reported [22]. For all of such processes, the optimum H₂:CO molar ratio would also depend on the process conditions and catalysts used.

Our previous work has investigated the production of a hydrogen-rich syngas from RDF using a two-stage pyrolysis-catalytic steam reforming process [23-26]. Pyrolysis of RDF alone produced a H₂:CO ratio of 0.7:1, however, introduction of steam and a 10 wt.% Ni-Al₂O₃ catalyst produced a H₂:CO ratio of 2.7:1 from the pyrolysis-catalytic steam reforming process [23]. In a later paper using SiO₂ as the support material, it was shown that the H₂:CO ratio could be manipulated from 1.3:1 - 3.4:1 depending on the composition of the catalyst and the catalyst preparation method [24]. Increased amounts of nickel (5wt.% - 40 wt.%) showed a linear increase in the H₂ yield and H₂:CO ratio and the addition of metal promoters (Ce, Mg, Al) to the Ni-SiO₂ had little influence on hydrogen yield or H₂:CO ratio.

Research on the production of hydrogen and syngas from wastes has concentrated on catalytic steam reforming, however, there is increasing work on the application of dry reforming using CO₂ as the reforming agent for syngas production from wastes and biomass [27-29]. The current interest in developing dry reforming is an attempt to utilise 'captured CO₂' which will be readily available should development of CO₂ capture and utilisation processes progress; thereby, mitigating the problems of climate change. However, catalytic dry reforming produces a lower yield of hydrogen and therefore, lower H₂:CO molar ratio compared to catalytic steam reforming, for example the CO₂ reforming of methane produces a syngas with a H₂:CO molar ratio of ~1:1 and steam reforming produces a H₂:CO ratio of

~4:1 [30]. Therefore, it is advantageous to combine CO₂ and steam catalytic reforming to manipulate the H₂:CO molar ratio to fit the specific end-use application required for the syngas. Such a process strategy has been investigated for the combined catalytic steam/CO₂ reforming for the production of syngas with a defined H₂:CO molar ratio. The co-reforming process has been studied extensively for methane [30-32], but also in relation to biomass [33-36] but less so in relation to wastes (plastics) [37]. Therefore, there is a need to extend the understanding of the combined catalytic steam and CO₂ reforming process for different types of feedstock, in particular in relation to different wastes, where development of the process opens up new higher value resource recovery options for the management of different wastes.

In this paper, we report on an experimental investigation of the combined catalytic steam and CO₂ reforming of processed municipal solid waste in the form of refuse derived fuel (RDF), with the aim of manipulating the H₂:CO molar ratio in the product syngas. As far as the authors are aware, this work represents for the first time that refuse derived fuel has been investigated in such a process. A two-stage pyrolysis-catalytic steam/CO₂ reforming reactor system was used with a 10 wt.% Ni-Al₂O₃ catalyst. The influence of process parameters including the steam:CO₂ ratio, the RDF to rate of steam/CO₂ input and catalyst temperature were studied in a wide range of experiments. Then, using the experimental data and Design of Experiments modelling, the influence and interdependency of the various variables investigated was determined to optimise the production of syngas and the H₂:CO molar ratio. The yield of gases, in particular H₂ and CO, and the syngas H₂:CO molar ratio are reported in relation to the process variables.

2. Materials and Methods

2.1 Refuse derived fuel

In this research, the processed municipal solid waste was in the form of refuse derived fuel (RDF) and was selected to be representative of municipal solid waste (MSW), but with the removal of recyclable glass and metals. RDF was chosen for this research rather than SRF, since being derived from MSW it has a similar composition to SRF I that it is mainly composed of a mixture of biomass and plastics, but is less regulated in terms of quality

specifications, thereby implying that RDF is less expensive to produce. It was produced by a UK materials recycling facility (Byker, UK) from unprocessed MSW with the final product being a pelletised refuse derived fuel. The RDF as received was in the form of pellets 40 mm in length and 20 mm in diameter, but were milled followed by sieving, resulting in particles in the size range $> 0.5 \leq 1$ mm for all experiments conducted. Proximate and elemental analysis of the RDF was undertaken using a Mettler Toledo TGA/DSC3+, to BS EN ISO standards and a Thermo Scientific Flash EA2000 elemental analyser to BS EN ISO standards respectively; the results are shown in Table 1.

2.2. Catalyst Preparation

The catalyst used in this work was a 10% Ni-Al₂O₃ catalyst, which is a commonly used reforming catalyst, due to its relatively low cost and reported effectiveness for the dry or steam reforming of biomass and plastics pyrolysis gases. The 10 wt.% Ni-Al₂O₃ catalyst used throughout this work was prepared by wet impregnation method containing 10% weight of metal nickel. Alumina oxide (Al₂O₃) (50-212 μ m) was used as the support and nickel (III) nitrate hexahydrate, Ni(NO₃)₂:6H₂O, provided the metal precursor. Chemicals were obtained from Sigma-Aldrich UK, Ltd. Ni(NO₃)₂:6H₂O was dissolved in deionised water followed by the addition of Al₂O₃ support material and stirred for a further 30 minutes. The solution was continually mixed for 4 h whilst slowly increasing the temperature until a semi-solid precipitate remained. The precipitate was dried overnight at 105 °C, then calcined at 750 °C with a heating rate of 20 °C per minute and held at 750 °C for three hours. The catalysts were then crushed and sieved to a 50-212 μ m particle size. Finally, the sieved catalysts were reduced in a 5% hydrogen and 95% nitrogen atmosphere at 800 °C with a heating rate of 20 °C min⁻¹ and held at 800 °C for two hours. Temperature programmed reduction (TPR) of the catalyst was carried out to ensure that the catalyst was fully reduced and the resultant TPR thermogram is shown in the Supplementary Information.

2.3. Experimental reactor system

The reactor system used for the two-stage pyrolysis-catalytic steam/CO₂ reforming of refuse derived fuel (RDF) is shown as a schematic diagram in Figure 1. The reactor was constructed

of stainless steel, and was 500 mm in length by 50 mm internal diameter. The two stages were externally heated using two separate 1.5 kW electrically heated furnaces, independently controlled and monitored by thermocouples. The RDF sample (2.0 g) was placed in a stainless steel crucible which was held centrally in the 1st stage pyrolysis reactor. The 10 wt.% Ni-Al₂O₃ catalyst was held in place centrally in the 2nd stage catalytic reactor supported on a stainless-steel metal gauze and quartz wool to produce a fixed bed of catalyst. The mass of catalyst:RDF ratio of between 0.5:1 — 2:1 was used depending on the experiment. Steam was introduced into the 2nd stage catalytic reforming reactor using water addition via a metered syringe pump. Carbon dioxide reforming gas was also introduced into the 2nd stage from a pressurised gas cylinder and metered using mass flow control. A total input reforming gas:RDF ratio of between 1.5:1 — 4:25:1 g hr⁻¹ was used depending on the experiment. The experimental procedure involved pre-heating the 2nd stage catalyst reforming reactor to the desired catalyst temperature and once stable, the pyrolysis stage was heated from 20 °C to 600 °C at 15°C min⁻¹ heating rate and then held for 30 minutes to allow for completion of the pyrolysis-catalytic steam/CO₂ reforming process. Nitrogen was used as a continuously flowing purge gas at 200 ml min⁻¹. Thereby, the evolved gases from the pyrolysis of the RDF were passed to the second catalytic stage where catalytic reforming of the evolved pyrolysis gases took place in the presence of steam/CO₂. Once both stages had reached their respective target temperatures, the product gases were passed through a condenser system consisting of air and dry-ice cooled condensers. The gases were collected in a 25 L Tedlar™ gas sample bag and analysed by off-line gas chromatography.

2.4. Syngas analysis

Three gas chromatography analysers were used to determine the concentration of the gases produced from the pyrolysis-catalytic reforming experiments. All columns had dimensions of 2 m length x 2 mm diameter. Permanent gases (H₂, O₂, N₂ and CO) were analysed using a Varian CP-3330 GC equipped with a thermal conductivity detector (TCD), with a HayeSep 60–80 mesh column, with argon as a carrier gas. Carbon dioxide was analysed using a Varian CP-3800 GC equipped with a thermal conductivity detector (TCD), with a HayeSep 80–100 mesh column, with argon as a carrier gas. Hydrocarbon gases (C₁ to C₄) were analysed using a

Varian CP 3380 GC equipped with a flame ionisation detector (FID), with a HayeSep 80–100 mesh column, with nitrogen as a carrier gas. The total mass of gas produced was determined from the gas chromatographic data; knowing the N₂ gas flow, experimental time and gas concentration in the gas sample bag, the mass of other gases could be calculated. Therefore the total gas yield could be determined by mass rather than ‘by difference’.

2.5. Catalyst characterization

The crystal structure of the catalysts was analysed by X-ray diffraction (XRD) using a Bruker D8 diffractometer, using a Cu-K α X-ray source at 40 kV and 40 mA with a Vantec position sensitive detector in the 2 θ range of 10 — 100°. The XRD patterns were analysed using High Score Plus software and the nickel crystal size calculated using the Scherrer equation. Thermogravimetric temperature programmed oxidation (TGA - TPO) using a Mettler Toledo TGA/DSC3+ was performed to measure the amount of carbon (coking) deposited on the used catalysts. A sample (~10 mg) was first degasified and heated from ambient temperature to 100 °C at 10 °C min⁻¹ in a N₂ stream with a dwell time of 10 minutes to stabilise, subsequently the gas was switched to air at 50 ml min⁻¹ flow rate and heated from 100 to 800 °C at 10 °C min⁻¹, with a dwell time of 10 minutes. Additionally the carbon content of the used catalysts was further quantified by a Thermo Scientific Flash EA2000 elemental analyser. The specific surface area, total pore volume and pore size was measured using a Micromeritics Tristar II 3000, prior to analysis the samples were degassed using a Micromeritics FlowPrep 060 at 200 °C in a N₂ stream. The specific surface area was calculated from the adsorption curve, using the Multipoint Brunauer, Emmett & Teller (BET) equation. The total pore volume and pore diameter were calculated using the Barrett, Joyner & Halenda (BJH) method.

2.6. Design of Experiments (DoE)

Design of Experiments modelling is a technique for understanding the inter-relationships of several different experimental parameters and is also used for process optimization. The modelling enables the maximum interpretation of the process variables to be obtained with a reduced number of experiments undertaken. Design of Experiments is an effective method

for optimizing processes based on polynomial surface analysis. It is a collection of mathematical and statistical techniques that are useful for the analysis in which an end-product of interest is influenced by several variables. For example, in this work, the H₂ yield, CO yield and H₂:CO ratio in the syngas are influenced by a range of parameters, including steam/CO₂ input ratio, catalyst reforming temperature, reforming gas:RDF ratio and catalyst:RDF ratio.

The pyrolysis-catalytic reforming of refuse derived fuel was investigated using a Design of Experiments (DoE) approach using the process conditions: catalytic reforming temperature (700-900 °C), (although additional experiments outside the design space for catalyst temperatures of 650 °C and 955 °C were also carried out (Supplementary Information)), (X₁); input reforming gas:RDF ratio (1.5:1 - 4.25:1 g hr⁻¹), (X₂); steam:CO₂ reforming gas ratio (75:25 - 25:75), (X₃) and catalyst:RDF ratio (0.5:1 – 2:1) (X₄) (Supplementary Information, Table S1). The wide range of experimental results (Supplementary Information, Table S2 and Figure S1) produced in relation to the different process variables using the two-stage experimental reactor system were analysed in the Design of Experiments Sartorius, Modde software. Models were fitted with multiple linear regression. Table 2 shows the analysis of variance (ANOVA) model data and Table 3 shows the DoE Equations 1 - 3 which show the relationship between the response function (i.e. H₂ yield, CO yield and H₂:CO ratio) and the process variables. All models for the response functions; H₂, CO and H₂:CO ratio were statistically significant indicated by their F-value and P-value of <0.001. High R² values for all models indicate an excellent fit of the data with residuals indicating the regression modelling procedure was acceptable and there was no lack of fit. The R² adjusted values are also acceptable indicating that the models are not overfitted. The Q² value (>0.1 for a significant model, > 0.5 for a good model) which indicates how well the model can predict new response values were either significant or good for all response variables. All models had coefficients terms analysed and removed to improve and optimise the Q² whilst still preserving high R² and R² adjusted values, this was achieved by removing some non-significant square and interaction terms. As indicated by the ANOVA analysis and DoE model equation coefficients the various process parameters have varying degrees of influence on the catalytic reforming of the pyrolysis gases and vapours affecting the syngas quality and quantity produced. The factor regression coefficients will either have

a synergistic or antagonistic influence on the response yield depending if a positive or negative value. Response surface plots were created to visualise and explore the factors and interactions on the response yields by varying two factors whilst keeping the other two factors at the central point.

3. RESULTS AND DISCUSSION

3.1. Influence of process variables on hydrogen yield

The data from the experiments investigating the two-stage pyrolysis-catalytic reforming of RDF in relation to the different process variables was analysed in relation to the yield of hydrogen coupled with Design of Experiments modelling. Table 3, DoE Equation 1 shows that the H₂ yield is a function of catalytic reforming temperature (X_1), input reforming gas:RDF ratio (X_2), steam:CO₂ reforming gas ratio (X_3), and catalyst:RDF ratio (X_4). The catalyst:RDF ratio (X_4) is the most significant influencing factor with a large positive correlation coefficient indicating a synergistic effect on H₂ yield, however the quadratic term is negative indicating an antagonistic effect at high catalyst:RDF ratio. The steam:CO₂ reforming gas ratio, (X_3), composition is additionally a significant influence on the H₂ yield with a positive first-order coefficient with a small negative quadratic term. Furthermore, the catalytic reforming temperature (X_1) is significant in its effect on the H₂ yield.

It is important to note the wide range and complexity of the reactions taking place in the two-stage, pyrolysis-catalytic steam/CO₂ reforming process [38]. The main reactions occurring during the pyrolysis-catalytic steam/CO₂ reforming of RDF are illustrated in Table 4. RDF consists of largely a mixture of biomass and plastics and the initial pyrolysis stage may be represented by pyrolysis of biomass and pyrolysis of plastics. The biomass components of RDF (paper, card, wood) are made up of different proportions of the oxygenated biopolymers, cellulose, hemicellulose and lignin. Cellulose is a carbohydrate (polysaccharide) with a linear polymer structure based on $\beta(1\rightarrow4)$ linked D-glucose, hemicellulose is also a carbohydrate (polysaccharide) but with a branched, cross-linked structure composed of several monomer sugars [39]. Lignin is a much more complex biopolymer with a three-dimensional alkyl-aromatic structure. The thermal degradation products identified from the pyrolysis of cellulose include, include, CO, CO₂ and H₂, and much more complex oxygenated

hydrocarbons such as levoglucosan, aldehydes, ketones and organic acids [39,40]. The thermal degradation of hemicellulose during the pyrolysis process produces CO, CO₂, H₂, C₁-C₂ hydrocarbons and oxygenated hydrocarbons such as organic acids and aldehydes. The thermal degradation of lignin produces mainly, CO, C₁ – C₂ hydrocarbons, and oxygenated hydrocarbons such as phenols, organic acids, alcohols and ketones. The pyrolysis of the biomass components in the RDF may be represented by Equation 1 (Table 4) where the pyrolysis process produces a range of thermal decomposition products including, H₂, CH₄ and CO, CO₂, hydrocarbons and oxygenated hydrocarbons, high molecular weight tars and residual char. The waste plastic composition of RDF will mostly be composed of polyethylene, polypropylene, polyethylene terephthalate and polystyrene. For example, the pyrolysis of a polyalkene, thermoplastic such as polyethylene involves the thermal degradation of the polymer chain through random scission of the bonds to produce mainly n-alkane hydrocarbons ranging from methane (C₁) to high molecular weight hydrocarbons (~C₆₀); in addition, lower concentrations of alkenes and alkadienes and also hydrogen are formed [41] (e.g. Equation 2). Polypropylene is also a polyalkene plastic and during pyrolysis, the plastic thermally degrades through random scission of the polymer bonds to also produce a range of low and high molecular weight alkanes, alkenes and alkadienes. Polyethylene terephthalate has a structure which includes linear, aromatic and oxygenated groups and scission of the polymer bonds during the pyrolysis process produces a range of compounds, including, terephthalic acid and benzoic acid and gaseous CO and CO₂. Polystyrene is a polymer including an aromatic ring and therefore produces different hydrocarbon fragments compared to the polyalkene plastics, instead, producing mainly styrene, but also other single ring aromatic compounds such as benzene, xylenes, toluene, alkylated benzenes and styrene oligomers [41]. Clearly, the pyrolysis of RDF produces a very complex mixture of hydrocarbons and oxygenated hydrocarbons. The product yield from the pyrolysis of the RDF, (without a second catalytic reforming stage), produced a product yield of 14 wt.% gases, 55 wt.% liquid and 31 wt.% char. For the two-stage, pyrolysis-catalytic steam/CO₂ reforming experiments, the liquids (55 wt.%) would not be condensed and therefore, would pass to the second stage as uncondensed vapours along with the gases (14 wt.%), representing 69 wt.% of volatile products of RDF pyrolysis. The uncondensed volatile pyrolysis products are passed by the nitrogen carrier gas to the high temperature second stage catalytic reactor where a further range of complex reactions takes place in the

presence of the steam and CO₂ reforming agents. For example, lighter hydrocarbons such as methane will undergo catalytic steam reforming reactions (Equations, 3 and 4) and catalytic CO₂ (dry) reforming (Equation 5) to produce hydrogen and carbon monoxide. The wide range of higher molecular weight hydrocarbons produced mainly from the pyrolysis of the plastics, will also undergo catalytic steam and CO₂ reforming to produce more hydrogen and carbon monoxide (Equations 6 and 7). The higher molecular weight oxygenated hydrocarbons will also be catalytic reformed by the steam and CO₂, (for example, Equation 8). The higher temperature conditions (700-900 °C), in the catalytic reactor will induce thermal and catalytic cracking of the hydrocarbon and oxygenated hydrocarbon fragments produced from pyrolysis of the biomass and plastic components; thereby, producing lighter hydrocarbons (CH₄, and C_nH_m), H₂, CO and CO₂ (Equation 9). These product hydrocarbons from the cracking reactions then undergoing catalytic steam and CO₂ reforming to produce further hydrogen and carbon monoxide. The complex reaction environment in the catalyst reactor may additionally involve (i) reactions between steam and carbon monoxide via the water gas shift reaction to produce more hydrogen (Equation 10); (ii) reactions between catalyst carbon deposits and steam to produce hydrogen via water gas reactions to produce hydrogen (Equations 11 and 12); (iii) reactions involving carbon and CO₂ via the Boudouard reaction to produce carbon monoxide (Equation 13).

The relationship between the independent variables and the H₂ yield can be explored and inferred from the response surface plots (RSP) derived from the DoE modelling of the experiments shown in Figure 2(a) - 2(f). The data shown in Figure 2(a) suggests that when the steam:CO₂ reforming gas ratio, comprises a higher CO₂ input (ratio 25:75) there is little influence of the catalytic reforming temperature and lower H₂ yields (~28.0 mmol g_{RDF}⁻¹) are produced. However, at higher steam:CO₂ ratios, where there is more steam available for reaction, the influence of the catalytic reforming temperature is more pronounced, such that at the steam:CO₂ ratio of 75:25, there is a marked increase in H₂ yield to ~40.0 mmol g_{RDF}⁻¹. This can be partly explained by the nature of the reactions taking place that favour higher temperatures due to their endothermic nature in the reforming process to produce H₂. Furthermore, the steam reforming reactions produce more moles of H₂ per unit than the dry reforming reaction.

Guillaume et al. [35] investigated CO₂ reforming and combined CO₂/steam reforming of biogas (66 vol.% CH₄; 34 vol.% CO₂) in the presence of a Ni-Rh/MgAl₂O₄ catalyst. They showed that methane reforming to produce hydrogen was increased with higher steam addition to the CO₂ reforming gas, leading to higher H₂:CO ratios. This was attributed to steam reforming of the CH₄ and water gas shift reaction of the CO₂ in the input feed biogas. They also attributed the higher effectiveness of steam compared to CO₂ as due to competitive adsorption of reactive species on the catalytic active sites. The H₂O being able to displace CO₂ leading to inhibition of the dry reforming reaction. Gao et al. [31] also reported that for the catalytic reforming of a methane/CO₂ mixture using a Ce-Ni/ZSM-5 catalyst, higher content of steam in the combined steam/CO₂ reforming gas produced a higher H₂:CO ratio and an inhibition of CO₂ conversion. They suggested that the addition of steam enhances the methane reforming reaction, but suppresses the CO₂ reforming reaction. Additionally, the water gas shift reaction between steam and CO produces more H₂ and CO₂ and is therefore unfavourable to CO₂ conversion. Xu et al. [33] compared dry and steam reforming of biomass (rice husks) pyrolysis gas in the presence of a Ni/Fe/Ce/Al₂O₃ catalyst in relation to a range of process parameters. They reported higher H₂:CO ratios in the presence of steam. Saad and Williams [37] investigated the two-stage, pyrolysis-steam/dry reforming of municipal solid waste plastics and reported that the input steam:CO₂ reforming gas ratio had a major influence on the H₂:CO molar ratio.

Figure 2(b) clearly shows that increasing the catalyst:RDF ratio has a positive effect on the H₂ yield, this suggests that there is increased availability of active sites for the pyrolysis gases and tars to be reformed. Furthermore, the curvature of the response surface plots of the catalyst:RDF and input reforming gas:RDF ratios can be seen, indicating that an optimal catalyst:RDF ratio is between 1.5:1 and 2:1 when inputting between 1.75:1 and 4.25:1 g hr⁻¹ of the reforming gases which produced a H₂ yield of ~35.0 mmol g_{RDF}⁻¹. Figure 2(c) shows the interaction between catalyst:RDF ratio and the catalytic reforming temperature indicating that the H₂ yield is reduced (~21.0 mmol g_{RDF}⁻¹) when the temperature is low (700 °C) and catalyst:RDF ratio is low (0.5:1). It can be seen that as the catalytic reforming temperature is increased or the catalyst:RDF ratio is raised there is an increase in H₂ yield, with an expected H₂ yield of ~36.0 mmol g_{RDF}⁻¹ when the catalyst:RDF loading is 1.5:1 to 1.75:1 and with a catalyst reforming temperature of 900 °C. However,

even at catalyst:RDF ratios between $\sim 1.25:1$ and $\sim 2:1$ and catalytic reforming temperatures above ~ 800 °C the H_2 yield is still ~ 34.0 mmol g_{RDF}^{-1} .

The steam and dry reforming reactions are endothermic (e.g. Table 4) and consequently, higher temperatures will favour these reforming reactions resulting in higher yields of hydrogen and higher $H_2:CO$ ratios. Xu et al. [33] compared dry and steam reforming of biomass (rice husks) pyrolysis gas and confirmed that the endothermic nature of the reforming reactions favoured higher H_2 and CO yield at higher temperature corresponding with enhanced reforming of hydrocarbons. Also, they reported a reduction of CO_2 concentration which was consumed in the dry reforming process. Gao et al. [31] investigated the influence of catalyst temperature between 650 °C and 800 °C with a Ce-Ni/ZSM-5 catalyst for the combined steam/ CO_2 reforming of biogas and also reported a linear increase in methane conversion and increased hydrogen production with an increase in catalyst temperature. In addition, Guilhaume et al., [35] also showed that at higher catalyst temperatures ($600 - 800$ °C), H_2O species were preferentially adsorbed on the catalyst surface compared to CO_2 and resulted in increased methane reforming and higher $H_2:CO$ ratios; the catalyst used was, Ni-Rh/ $MgAl_2O_4$.

Figure 2(d) shows the input reforming gas:RDF ratio and the influence of catalytic reforming temperature on the H_2 yield. It may be suggested that catalytic reforming temperature is the more influential factor, as increasing the catalytic reforming temperature at all values of the input reforming gas:RDF ratio increases the H_2 production, achieving a H_2 yield of ~ 36.0 mmol H_2 g_{RDF}^{-1} . It is also apparent that the input reforming gas:RDF ratio has curvature, suggesting that the lowest ($1.75:1$ g hr^{-1}) and highest ($4.25:1$ g hr^{-1}) input reforming gas:RDF ratios will correspond to lower H_2 yields with an optimal range between the lowest and highest values at any given catalytic reforming temperature. The response surface plots (Figure 2(e)) of steam: CO_2 reforming gas ratio and catalyst:RDF ratio, shows that when the steam: CO_2 reforming ratio is greater than $50:50$, i.e. with higher input steam, H_2 production is favoured and also when the catalyst:RDF ratio is increased from $0.5:1$ to $2:1$. This can be attributed to the steam reforming reaction dominating, thereby, producing more H_2 than the corresponding dry reforming reaction. Additionally, increased catalyst:RDF ratio allows for more RDF pyrolysis gases and tars to interact with active sites on the catalyst surface thus more reforming can occur resulting in a higher H_2 yield of ~ 38.0 mmol g_{RDF}^{-1} .

Figure 2(f) indicates that the input reforming gas:RDF ratio has little influence on the H₂ yield when the input steam:CO₂ reforming gas composition is mainly CO₂, however as steam becomes the main fraction of the input reforming gas composition, the amount of steam input into the reactor system influences the H₂ yield with an optimal input reforming gas :RDF ratio range of around ~2:1 to ~3.5:1 g hr⁻¹ with H₂ production reaching ~36.0 mmol g_{RDF}⁻¹.

Gao et al., [31] also reported only a negligible influence of reforming gas (steam:CO₂) input flow rate for the combined steam and dry reforming of biogas (CH₄/CO₂), however, at very high input gas flow rates, methane conversion was reduced and CO₂ conversion was increased. Xu et al. [33] also reported that there is an optimum reforming gas input flow rate for both dry reforming and steam reforming with reduced production of hydrogen at low and high reforming gas input flow rates for the reforming of biomass pyrolysis gas. This was attributed to limited mass transfer of reactants and kinetic control of different reactions at low and high flow rates.

Overall, from the Design of Experiments response surface plots based on the extensive experimental work carried out in this work, it may be suggested that H₂ production is favoured when the catalytic reforming temperature is greater than 800 °C, input reforming gas:RDF ratio is between ~2:1 and ~3.5:1 g hr⁻¹, the steam:CO₂ reforming gas ratio composition is 50:50 (or more towards steam) and catalyst:RDF loading ratio is around 1.5:1.

3.2. Influence of process variables on carbon monoxide yield

The data from the experiments investigating the two-stage pyrolysis-catalytic reforming of refuse derived fuel in relation to the different process variables was analysed in relation to the yield of carbon monoxide coupled with Design of Experiments modelling. As indicated by the regression equation (Table 3, DoE Equation 2) the main influencing factor on the yield of carbon monoxide is the composition of the steam:CO₂ reforming gas ratio with its negative term. Thus, when the steam:CO₂ reforming gas composition contains more steam, there is a reduction in CO yield. Conversely, increases in the catalytic reforming temperature or the catalyst:RDF ratio to the system causes CO yield to increase as indicated by their positive values.

The DoE response surface plots shown in Figure 3(a) - 3(f) show the production of CO in relation to the various process variables produced from the RDF pyrolysis-catalytic reforming experiments. The results show how the factors (variables) influence the CO yield and any interactions between them. Figure 3(a) shows the influence of the catalyst:RDF ratio and the influence of the input reforming gas:RDF ratio. It is apparent from the results that when the catalyst:RDF ratio is at the lowest (0.5:1) the amount of CO produced is at a minimum ($\sim 12.0 \text{ mmol g}_{\text{RDF}}^{-1}$), furthermore, an increase in the input reforming gas:RDF ratio has little influence on CO production. As the catalyst:RDF ratio increased from 0.5:1 to 2:1, the CO production increased markedly with a potential CO yield of $\sim 19.0 \text{ mmol g}_{\text{RDF}}^{-1}$. Again, the amount of input reforming gas:RDF ratio has only a small effect on CO production, with a small decrease in CO production at the highest catalyst:RDF ratio and highest input reforming gas:RDF ratio.

The DoE response surface plots produced from the Design of Experiments modelling based on the experimental data of the influence of the amount of catalyst:RDF ratio and the catalytic reforming temperature are shown in Figure 3(b). The results show that the small CO yield ($\sim 7.7 \text{ mmol g}_{\text{RDF}}^{-1}$) is obtained at low catalyst:RDF ratio (0.5:1) and low catalytic reforming temperature ($700 \text{ }^\circ\text{C}$). But, with increasing catalyst:RDF ratio and increased catalytic reforming temperature, CO production is significantly increased to $\sim 22.0 \text{ mmol g}_{\text{RDF}}^{-1}$. This would be expected due the endothermic reforming processes taking place favouring higher temperatures and greater availability of active sites on the catalyst for reforming to occur.

The influence of input reforming gas:RDF ratio and catalytic reforming temperature (Figure 3(c)) shows how the catalytic reforming temperature has a significant influence on the CO yield whilst the input reforming gas:RDF ratio has little influence. The increasing CO production is predicted with a reforming gas:RDF ratio between 2.5:1 to 3.5:1 g hr^{-1} at all catalytic reforming temperatures, with the highest yield of $\sim 22.0 \text{ mmol g}_{\text{RDF}}^{-1}$. Figure 3(d) shows the influence of changing the steam:CO₂ reforming gas ratio on CO production in relation to the catalyst:RDF ratio. The results indicate that the CO yield is high ($\sim 27.0 \text{ mmol g}_{\text{RDF}}^{-1}$) when the steam:CO₂ reforming ratio is comprised of mainly CO₂, and increasing the catalyst:RDF ratio enhances the CO yield. This can be explained by the dry reforming reaction producing two moles of CO (Table 4, Equation 5) compared to the steam reforming

reaction which produces only one mole of CO (Table 4, Equation 3). Conversely, when the steam:CO₂ reforming gas composition ratio is mainly steam, the CO yield is reduced ($\sim 9.8 \text{ mmol g}_{\text{RDF}}^{-1}$), this may be due to an excess of steam leading to oxidation of carbon to produce H₂ and CO₂. Similarly, Figure 3(e) also shows the influence of changing the steam:CO₂ reforming gas composition in relation to the input reforming gas:RDF ratio where a low CO yield is produced at higher steam reforming gas content.

The DoE response surface plots of the experiments in relation to the steam:CO₂ reforming gas ratio and the influence of the catalyst reforming temperature on CO yield is shown in Figure 3(f). At low catalytic reforming temperature (700 °C) with steam dominating the steam:CO₂ reforming gas composition, the CO production is reduced ($\sim 9.4 \text{ mmol g}_{\text{RDF}}^{-1}$). Increasing the catalytic reforming temperature at higher steam inputs has a positive effect on CO production increasing to $\sim 16.0 \text{ mmol g}_{\text{RDF}}^{-1}$. Conversely when the steam:CO₂ reforming gas ratio is comprised of mainly CO₂, at low catalytic reforming temperature, the CO yield ($\sim 18.0 \text{ mmol g}_{\text{RDF}}^{-1}$) is greater than at the corresponding steam composition. Whereas, at high catalytic reforming temperature (900 °C) the CO yield is significantly higher, reaching $\sim 30.0 \text{ mmol g}_{\text{RDF}}^{-1}$. This can be explained by the two different reactions taking place with dry reforming producing more CO than steam reforming and the reactions favouring higher temperatures. Xu et al. [33] and Guilhaume et al., [35] have also shown that increased catalyst temperature promotes hydrocarbon reforming reactions leading to increased H₂ and CO due to the endothermic nature of the dry and steam reforming reactions.

Overall, from the experimental data supported by DoE modelling response surface plots it could be suggested that CO production is favoured when the catalytic reforming temperature is over 800 °C, the input reforming gas:RDF ratio is between $\sim 2:1$ and $\sim 3.75:1 \text{ g hr}^{-1}$, the steam:CO₂ reforming gas ratio composition is 50:50 (or more towards CO₂) and the catalyst:RDF ratio is $\sim 1.5:1$ to $2:1$.

3.3. Influence of process variables on syngas H₂:CO ratio

The data from the experiments investigating the two-stage pyrolysis-catalytic reforming of RDF in relation to the different process variables was analysed in relation to the syngas yield, i.e. the ratio of H₂:CO, and plotted as DoE surface response plots derived from the Design of

Experiments model. The results presented as DoE response surface plots are shown in Figure 4(a) - 4(f). The regression equation for H₂:CO ratio (Table 3, DoE Equation 3) indicates the steam:CO₂ reforming gas ratio has the greatest influence on the H₂:CO ratio with an increasing trend as the composition has a greater amount of steam to CO₂. The coefficients with liner terms X₁, X₂, X₃ and interaction terms X₁, X₂ and X₂, X₃ were found to be significant.

The DoE response surface plots shown in Figure 4(a), 4(b) and 4(d) show clearly that the amount of catalyst present in the catalytic reforming reactor is not a major influencing factor on the molar ratio of H₂:CO in the product syngas for all catalyst:RDF ratios investigated here. However, Figure 4(a) shows that increasing the input reforming gas:RDF ratio leads to higher H₂:CO molar ratio, and Figure 4(b) suggests that lower catalytic reforming temperature favours a higher H₂:CO molar ratio. Also, affecting the syngas H₂:CO ratio is the steam:CO₂ reforming gas ratio, where changing the reforming gas from CO₂-rich to a steam-rich reforming gas composition changes the H₂:CO molar ratio from ~1.1:1 to ~2.9:1.

Figure 4(c) shows the DoE response surface plots of the experimental data from the pyrolysis-catalytic reforming of RDF in relation to the catalytic reforming temperature and the influence of input reforming gas:RDF ratio. Above a catalyst temperature of ~800 °C the input reforming gas:RDF ratio has little influence on the H₂:CO ratio, resulting in a low H₂:CO molar ratio. But, at lower catalyst temperatures (below ~800°C) both the catalytic reforming temperature and the input reforming gas:RDF ratio influence the H₂:CO molar ratio. For example, with a input reforming gas:RDF ratio of 1.75:1 g hr⁻¹ and catalytic reforming temperature of 700°C, the H₂:CO ratio produced is 2.2:1 and at the same catalytic reforming temperature of 700°C but with an input reforming gas:RDF ratio of 4.25:1 g hr⁻¹ the ratio increases to 2.8:1.

The steam:CO₂ reforming gas ratio has the greatest influence on the H₂:CO molar ratio, as shown in Figure 4(d), 4(e) and 4(f). Changing steam:CO₂ reforming gas ratio from a higher CO₂ input to a higher steam input clearly produces an increase in the H₂:CO molar ratio, which can be attributed to the different reforming reactions of the CO₂, steam/CO₂ and steam reforming gas. At higher CO₂ content in the reforming gas (mainly dry reforming), the product H₂:CO ratio is ~1:1, for steam/CO₂ (50:50 ratio) co-reforming the ratio produced is ~2:1 and for higher steam content in the reforming gas the product H₂:CO ratio is ~3:1.

However, as the input reforming gas:RDF ratio into the process is increased (Figure 4(e)) the H₂:CO molar ratio is also altered, for example, at higher CO₂ content, increasing input reforming gas:RDF ratio reduces the H₂:CO ratio and conversely, at higher steam input in the reforming gas, increased reforming gas:RDF ratio increases the H₂:CO ratio.

The DoE response surface plots for the pyrolysis-catalytic reforming of RDF in relation to the influence of the catalytic reforming temperature (Figure 4(f)) shows that the influence of the reforming temperature has a moderate effect when the reforming gas has a higher CO₂ content. For example, increasing the catalytic reforming temperature reduces the H₂:CO molar ratio from 1.5 at 700°C to ~0.9 mmol g_{RDF}⁻¹ at 900°C. The influence of the catalytic reforming temperature increases as the content of steam in the steam:CO₂ reforming gas ratio is increased, with a H₂:CO molar ratio of ~3.7:1 at an input steam:CO₂ ratio of 75:25 and a catalyst temperature of 700 °C.

3.4. Model validation and process optimisation

To validate the Design of Experiments model and to determine if the product syngas H₂:CO molar ratio could be manipulated in relation to targeted ratios optimised for end-use syngas applications were investigated. Target ratios of H₂:CO of 1:1 and 2:1 were selected. The modelling used a H₂:CO molar ratio within the target range between 0.9:1 – 1.1:1 (representing 1:1) and H₂:CO molar ratio within the target range of 1.7:1 and 2.2:1 (representing 2:1). The target ratios were selected based on the end-use requirements of the syngas, for example, a H₂:CO molar ratio of 1:1 is required for the production of aldehydes and dimethyl-ether [20,22] and a molar ratio of ~2:1 is typically used for Fischer Tropsch synthesis of liquid fuels [17] and for the synthesis of methanol [16]. The targeted H₂:CO molar ratios were input into the Modde Design of Experiments software which performed numerous calculations to determine the optimal factor levels of the variables to use along with the predicted response values.

The experimental conditions for the target H₂:CO molar ratio of 1:1 and 2:1 are shown in Table 5. The experiments were carried out using the two stage, pyrolysis-catalytic steam/dry reforming experimental reactor system. Experiments were performed in triplicate. The results of the Design of Experiments predictions from the Modde software

and the experimental validation results are shown in Figure 5 for the target 1:1 syngas H₂:CO molar ratio and in Figure 6 for the target 2:1 syngas H₂:CO ratio. Figure 5 shows that the predicted yield of gases from the model set up to produce a targeted H₂:CO molar ratio of 1:1, produced a H₂ yield of 29.5 mmol g_{RDF}⁻¹ and a CO yield of 27.3 mmol g_{RDF}⁻¹. This is in close agreement with the average experimental results from the pyrolysis-catalytic reforming reactor which produced a H₂ yield of 31.0 and a CO yield of 27.3 mmol g_{RDF}⁻¹. Figure 5 also shows that the H₂:CO ratio predicted from the model was 1.08:1, whereas the experimental data showed a slightly higher average H₂:CO molar ratio of 1.1:1. Figure 6 shows that for the target model prediction of a H₂:CO molar ratio of 2:1, the predicted H₂ yield was 34.0 mmol g_{RDF}⁻¹ and CO yield was 16.5 mmol g_{RDF}⁻¹. Again, the experimental data from the pyrolysis-catalytic reforming experiments produced H₂ and CO yields close to that predicted from the DoE model, with an average H₂ yield of 32.0 mmol g_{RDF}⁻¹ and CO yield of 15.1 mmol g_{RDF}⁻¹. The predicted H₂:CO molar ratio from the model was 2.0 and the experimental data again produced a slightly higher H₂:CO molar ratio of 2.15:1. The syngas H₂:CO ratios produced from the experimental pyrolysis catalytic reforming were slightly above the predicted values from the Design of Experiments Modde software. However, in the two-stage pyrolysis catalytic reforming process, there are numerous complex reactions that are simultaneously taking place. Therefore, the results of the validation and optimisation indicate the design of experiment model can predict the yield of gases from the experimental pyrolysis-catalytic dry/steam reforming process to an acceptable level. Furthermore, it may be concluded that refuse derived fuel as a feedstock for the pyrolysis-catalytic reforming process can be used to produce syngas with targeted H₂:CO molar ratios.

3.5. Catalyst Stability

To evaluate the stability of the 10 wt.% Ni-Al₂O₃ catalyst used as the reforming catalyst for the pyrolysis-catalytic steam/dry reforming of RDF, a series of repeat experiments were performed using the two validation and optimisation target parameters of H₂:CO molar ratio of 1:1 and H₂:CO molar ratio of 2:1. The experiments were performed without replacing the catalyst in the second stage catalytic reactor but with reloading of RDF into the first stage pyrolysis reactor. The results are presented in Figure 7 for the experiments aimed at producing a H₂:CO molar ratio of 1:1 and Figure 8 for the experiments aimed at producing a

H₂:CO molar ratio of 2:1. Figure 7 shows that the first experiment with the fresh 10 wt.% Ni-Al₂O₃ catalyst produced a high yield of both H₂ and CO, at 33.1 mmol g_{RDF}⁻¹ and 28.7 mmol g_{RDF}⁻¹ respectively and a H₂:CO molar ratio of 1.15:1. However, subsequent experiments resulted in significantly lower syngas production with the H₂ yield, reducing and stabilising at ~20.7 mmol g_{RDF}⁻¹ and CO yield reducing and stabilising at ~18.8 mmol g_{RDF}⁻¹. However, the H₂:CO molar ratio remained in the target range of ~1:1 varying between 1.09:1 and 1.11:1.

Figure 8 shows the results for the target model H₂:CO molar ratio of 2:1, which shows that the fresh catalyst produced a high yield of H₂ of 34.8 mmol g_{RDF}⁻¹ and a CO yield of 17.1 mmol g_{RDF}⁻¹ with a H₂:CO molar ratio of 2:1. However, the repeated experiments with the same catalyst in place produced a significantly reduced H₂ yield, reducing from 34.8 to 22.3 mmol g_{RDF}⁻¹ and subsequently stabilised at ~19.0 mmol g_{RDF}⁻¹. The yield of CO reduced from 17.1 to 10.8 mmol g_{RDF}⁻¹ and stabilised at ~9.0 mmol g_{RDF}⁻¹. However, the H₂:CO molar ratio remained in the target range of ~2:1 varying between 2.04:1 and 2.1:1 over the stability experiments. This reduction in syngas production is most likely attributed to the catalyst deactivating due to coking whereby the active metal sites have become either blocked or encapsulated with carbon preventing the pyrolysis gas and tars access to the active nickel sites to be reformed. Catalyst deactivation may also be due to sintering of the nickel particles whereby they have agglomerated together forming large particles thus hindering reforming opportunities.

3.6 Catalyst characterisation

The fresh and spent 10% Ni-Al₂O₃ catalysts after use were characterised before and after the pyrolysis-catalytic reforming of RDF for the experiments using the targeted experimental conditions shown in Table 5, relating to the data presented in Figures 5 for the target H₂:CO ratio of 1:1 and Figure 6 for the target ratio of 2:1. Also analysed were the used catalysts produced from the catalyst stability tests relating to the data presented in Figure 7 and Figure 8 for the different H₂:CO target ratios. The catalysts were characterised in relation to catalyst surface area and porosity and to metal particle size (Table 6) and in relation to crystal structure by XRD analysis (Figure 9). Figure 9 shows the XRD diffraction peaks at 2θ = 44°, 52°, 76°, 92° and 98° in the reduced fresh catalyst are attributed to crystalline Ni phases, which correspond to (1 1 1), (2 0 0), (2 2 0), (3 1 1) and (2,2,2) planes, respectively.

Furthermore, typical diffraction peaks corresponding to the Al_2O_3 catalyst support material are also detected at $2\theta = 19^\circ, 32^\circ, 37^\circ, 45^\circ, 60^\circ, 67^\circ$ and 85° . The nickel particle size was determined using the Scherrer equation, and as can be seen from Table 6 the fresh catalyst had a nickel particle size of 15.8 nm, but for the used catalysts the nickel particle size increased up to 33.2 nm indicating that agglomeration/sintering of the nickel particles has taken place. Furthermore, the XRD diffraction profiles of the spent catalysts did not show a peak at $2\theta = 26^\circ$, which is associated with carbon, thus suggesting catalyst deactivation was not attributed to coking.

The TPO data in relation to the used catalysts (Table 6 and Supplementary Information Figure S2) indicated that there was minimal coking of the catalysts used for the individual target $\text{H}_2:\text{CO}$ molar ratios of 1:1 and 2:1 and after the catalyst stability testing no carbon on the catalysts was detected by TPO. However, due to the oxidation of nickel this can obscure low temperature carbon therefore carbon elemental analysis was conducted to confirm the amount of carbon deposited on the catalysts. The results (Table 6) confirm the catalysts suffered from little carbon deposition, indicating that the decrease in activity of the catalyst is due to sintering and not catalyst carbonaceous coke formation.. The specific surface area, pore volume and pore size data (Table 6) supports sintering as the main reason for the decrease in activity as the surface area of the spent catalysts is markedly reduced, and the average pore size has increased. This may be attributed to the nickel particles agglomerating together forming large particles thus partially blocking pores and reducing the availability of the pyrolysis gases to be reformed due to less availability of active sites. The most likely reasons for the catalyst deactivation due to sintering is related to the high catalytic reforming temperature and the presence of steam in the reforming atmosphere used in this study both of which greatly increases the sintering process [42].

The work reported here has shown that the pyrolysis-catalytic steam/dry reforming of secondary recovered fuel produced from municipal solid waste is a process with potential for producing a syngas where the product H_2 and CO could be manipulated to produce a ratio targeted at a particular end-use application. However, there are some considerations of the process system that should be discussed. RDF is comprised of mainly biomass components and a mixture of plastics. There have been studies on the interaction of biomass and plastics during the pyrolysis process, which occurs in the first stage reactor used in this work. The biomass biopolymers hemicellulose, cellulose and lignin decompose during

pyrolysis over the temperature ranges of 200 °C — 330 °C, 330 °C — 450 °C, 250 °C — 550 °C respectively [39]. The main plastics in RDF also thermally decompose at different temperatures, for example, polyethylene and polypropylene between 430 °C — 520 °C, polyethylene terephthalate between 370 °C — 460 °C and polystyrene between 410 °C — 470 °C [6,43]. Therefore, interaction between RDF components during pyrolysis will be linked to their overlapping decomposition temperature regimes. For example, Li et al. [44] investigated the pyrolysis of hemicellulose and polyethylene using thermogravimetric analysis and reported no interaction between the components because of their different decomposition temperature ranges. Similarly, Gunasee et al. [45] reported no interaction between cellulose and polyethylene due to their different decomposition temperature regimes. However, Oyedun et al. [46] reported significant interaction between polystyrene and the lignin component of biomass since their pyrolysis decomposition temperatures were similar. The close intermingling of the biomass and plastic components can influence decomposition since it has been suggested that the release of radicals from biomass components during thermal degradation may interact with the plastic polymers initiating depolymerisation [47]. It has also been reported that the residual char formed from cellulose decomposition can react synergistically with the decomposition of polyethylene [45].

There is also the potential for interaction of the volatiles derived from the biomass and plastic components during the second stage catalytic reforming reactor used in the two-stage reactor system. For example, Akubo et al [48]. reported that lignin/plastics (polyethylene, polystyrene) mixtures produced higher hydrogen yields than cellulose/plastics mixtures from two-stage pyrolysis-catalytic steam reforming experiments. However, it is difficult to separate the interaction during the pyrolysis stage with the catalytic reforming stage in the work reported here. In the work reported here, the pyrolysis of the RDF consisted of heating the RDF at 15 °C per minute heating rate from 20 °C to 600 °C, representing a time of ~35 minutes, followed by a hold time of 30 minutes to ensure release of volatiles, i.e. a total time of ~1 hour. Therefore, in the process configuration used here, the pyrolysis stage will release a different suite of volatiles from the different biomass components and plastics over the time taken for the raising of the pyrolysis temperature which then pass at different times to the catalytic reforming stage.

4. CONCLUSIONS

The pyrolysis-catalytic reforming of RDF was found to be a suitable feedstock to produce a targeted syngas with a H₂:CO molar ratio suitable for further synthesis in Fischer-Tropsch, methanol or hydroformylation production. The composition of the syngas in terms of hydrogen, carbon monoxide and H₂:CO molar ratio was able to be successfully manipulated by varying the input rate of the reforming steam/CO₂ reforming gas, the steam and CO₂ composition of the reforming gas and temperature of the catalytic reforming reactor. The optimisation process was achieved by using a Design of Experiments approach which enabled a larger experimental design space to be explored whilst keeping the number of experiments to a reasonable amount. In addition, an additional benefit of modelling the results was to be able to predict new parameters to test for optimal results. The Design of Experiments (DoE) modelling used the experimental data to identify the process conditions that would produce a target syngas H₂:CO molar ratio of 1:1 and 2:1. The experimental results obtained at the optimised process conditions validated the model. The 10 % nickel alumina supported catalyst was found to be highly effective at the reforming of volatiles from the pyrolysis-catalytic reforming of RDF; producing a highest syngas yield of 67.4 mmol g_{RDF}⁻¹ and within target H₂:CO molar ratios of 1.7:1 -2.2:1 and 0.9-1.1 with a yield of H₂ of 51.9 mmol g_{RDF}⁻¹ and a yield of CO of 61.8 mmol g_{RDF}⁻¹. However, catalyst deactivation was observed with an approximate reduction in catalyst activity of 30% after one repeat experiment then stabilised at ~40 – 50% over 5 repeat experiments. Catalyst deactivation was attributed to metal particle sintering rather than catalyst carbonaceous coke formation.

Acknowledgements

We gratefully acknowledge the support of the UK Engineering & Physical Science Research Council (EPSRC) for a research scholarship for TKP via the EPSRC Centre for Doctoral Training in Bioenergy (EP/L014912/1).

REFERENCES

- [1] Goyal H.B., Seal D., Saxena R.C., Bio-fuels from thermochemical conversion of renewable resources: A review, *Renewable and Sustainable Energy Reviews*, 12, 2. Pergamon, 504–517, 2008.
- [2] European Commission Eurostat Waste Statistics (2019, Data) EUROSTAT, Brussels, 2021.
- [3] Tiseo I. Municipal solid waste in the US: Statistics and facts. Statista Inc., New York, US, 2021.
- [4] European Commission, “Refuse Derived Fuel, Current Practice and Perspectives,” European Commission, Brussels, 2003.
- [5] IEA (International Energy Agency) Bioenergy Task 36; Trends in the use of solid recovered fuels, 2020.
- [6] Gerassimidou S., Velis C.A., Williams P.T., Komilis D. Characterisation and composition identification of waste-derived fuels obtained from municipal solid waste using thermogravimetry: A review. *Waste Management & Research*, 38(9), 942-965, 2020.
- [7] Maitlo G., Mahar R., Bhatti Z.A., Unar I.N., A comprehensive literature review of thermochemical conversion of biomass for syngas production and associated challenges. *Mehran University Research Journal of Engineering & Technology*, 38,(2), 496-512, 2019
- [8] Rauch, R., Hrbek, J., Hofbauer, H., Biomass gasification for synthesis gas production and applications of the syngas, *Wiley Interdisciplinary Reviews: Energy and Environment*, 3, 343-362, 2014.
- [9] Molino, A., Chianese, S., Musmarra, D., Biomass gasification technology: the state of the art overview, *Journal of Energy Chemistry*, 25, 10-25, 2016.
- [10] Varank G., Ongen A., Guvenc S.Y., Ozcan H.K., Ozbas E.E., Guven E., Modeling and optimisation of syngas production from biomass gasification. *International Journal of Environmental Science and Technology*, 2021 (<https://doi.org/10.1007/s13762-021-03374-3>)
- [11] Alnouss A., McKay G., Tareq A., Production of syngas via gasification using optimum blends of biomass. *Journal of Cleaner Production*, 242, Article #118499, 2020.
- [12] Alasadi M., Miskolczi M., Hydrogen rich products from waste HDPE/LDPE/PP/PET over Me/Ni-ZSM-5 catalysts combined with dolomite. *Journal of the Energy Institute*, 96, 251-259, 2021.

- [13] Zhang S., Zhu S., Zhang H., Liu X., Xiong Y. High quality H₂-rich syngas production from pyrolysis-gasification of biomass and plastic wastes by Ni-Fe@Nanofibers/Porous carbon catalyst. *International Journal of Hydrogen Energy*, 44(48), 26193-26203, 2019.
- [14] Yao D., Yang H., Chen H. Williams P.T., Investigation of nickel impregnated zeolite catalysts for hydrogen/syngas production from the catalytic reforming of waste polyethylene. *Applied Catalysis B-Environmental*, 227, 477-487, 2018.
- [15] Kordoghli S., Khiari B., Paraschiv M., Zagrouba F., Tazerout M. Production of hydrogen and hydrogen-rich syngas during thermal catalytic supported cracking of waste tyres in a bench-scale fixed bed reactor. *International Journal of Hydrogen Energy*, 44(22), 11289-11302, 2019.
- [16] Song X., Guo Z., Technologies for direct production of flexible H₂/CO synthesis gas. *Energy Conversion & Management*, 47(5), 560–569, 2006.
- [17] Majewski A.J., Wood J., Tri-reforming of methane over Ni@SiO₂ catalyst. *Int. J. Hydrogen Energy*, 39(24), 12578–12585, 2014.
- [18] Cao Y. et al., Synthesis Gas Production with an adjustable H₂/CO ratio through the coal gasification process: effects of coal ranks and methane addition, *Energy & Fuels*, 22(3), 1720–1730, 2008.
- [19] Aasberg-Petersen A. et al., Synthesis gas production for FT synthesis, *Studies in Surface Science and Catalysis*, 152, 258–405, 2004.
- [20] Luk H.T., Mondelli C., Ferré D.C., Stewart, J.A. Pérez-Ramírez J. Status and prospects in higher alcohols synthesis from syngas,” *Chem. Soc. Rev.*, 46(5), 1358–1426, 2017.
- [21] Spath P.L., Dayton D.C., Preliminary Screening - Technical and economic assessment of synthesis gas to fuels and chemicals with emphasis on the potential for biomass-derived syngas, NERL, Golden, CO (United States), 2003.
- [22] Huang M.H., Lee H.M., Liang K.C., Tzeng C.C., Chen W.H. An experimental study on single step dimethyl-ether (DME) synthesis from hydrogen and carbon monoxide under various catalysts. *International Journal of Hydrogen Energy*, 40 13583-13593, 2015.
- [23] Blanco P.H., Wu C., Onwudili J.A., Williams P.T., Characterisation of tar from the pyrolysis/gasification of refuse derived fuel: Influence of process parameters and catalysis. *Energy & Fuels*, 26, 2107-2115, 2012.
- [24] Blanco P.H., Wu C., Onwudili J.A., Williams P.T., Characterization and evaluation of Ni/SiO₂ catalysts for hydrogen production and tar reduction from catalytic steam pyrolysis-reforming of refuse derived fuel. *Applied Catalysis B: Environmental*, 135, 238– 250, 2013.

- [25] Blanco P.H., Wu C., Onwudili J.A., Dupont V., Williams P.T. Catalytic pyrolysis/gasification of refuse derived fuel for hydrogen production and tar reduction: Influence of nickel to citric acid ratio using Ni/SiO₂ catalysts. *Waste & Biomass Valorization*, 5, 625-636, 2014.
- [26] Blanco P.H., Wu C. Williams P.T. Influence of Ni/SiO₂ catalyst preparation methods on hydrogen production from the pyrolysis/reforming of refuse derived fuel. *International Journal of Hydrogen Energy*, 39, 5723-5732, 2014.
- [27] Saad J.M., Williams P.T. Catalytic dry reforming of waste plastics from different waste treatment plants for production of synthesis gases. *Waste Management*, 58, 214-220, 2016.
- [28] Saad J.M., Williams P.T. Pyrolysis-catalytic dry (CO₂) reforming of waste plastics for syngas production; Influence of process parameters. *Fuel* 193, 7-14, 2017.
- [29] Colmenares J.C., Quintero R.F.C., Pieta I.S. Catalytic dry reforming for biomass-based fuels processing: Progress and future perspectives. *Energy Technology*, 4(8), 881-890, 2016.
- [30] Luyben W.L. Control of parallel dry methane and steam reforming processes for Fischer-Tropsch syngas. *Journal of Process Control*, 39, 77-87, 2016
- [31] Gao N.B., Cheng M.X., Quan C., Zheng Y.P. Syngas production via combined dry and steam reforming of methane over Ni-Ce/ZSM-5 catalyst. *Fuel*, 273, #117702, 2020.
- [32] Summa P., Samojeden B., Motak M. Dry and steam reforming of methane: Comparison and analysis of recently investigated catalytic materials. *Polish Journal of Chemical Technology*, 21(2) 31-37, 2019.
- [33] Xu X., Jiang E., Wang M., Xu Y. Dry and steam reforming of biomass pyrolysis gas for rich hydrogen gas. *Biomass and Bioenergy*, 78, 6-16, 2015.
- [34] Feng D.D., Zhao Y.J., Zhang Y., Sun S.Z., Effects of H₂O and CO₂ on the homogeneous conversion and heterogeneous reforming of biomass tar over biochar. *International Journal of Hydrogen Energy*, 42(18), 13070-13084, 2017.
- [35] Guillaume N., Bianchi D., Wandawa R.A., Yin W., Schuurman Y., Study of CO₂ and H₂O adsorption competition in the combined dry/steam reforming of biogas. *Catalysis Today*, 375, 282-289, 2021.
- [36] Schiaroli N., Volanti M., Crimaldi A., Passarini F., Vaccari A., Fornasari G., Coplelli S., Florit F., Lucarelli C. Biogas to syngas through the combined steam/dry reforming process: An environmental impact assessment. *Energy & Fuels*, 35(5), 4224-4236, 2021.
- [37] Saad J.M., Williams P.T. Manipulating the H₂/CO ratio from dry reforming of simulated mixed waste plastics by the addition of steam. *Fuel Processing Technology*, 156, 331-338, 2017.

- [38] Guan G., Kaewpanha M., Hao X., Abudula A., Catalytic steam reforming of biomass tar: Prospects and challenges. *Renewable and Sustainable Energy Reviews*, 58, 450-461, 2016.
- [39] Akubo K., Nahil M.A., Williams P.T., Pyrolysis-catalytic steam reforming of agricultural biomass wastes and biomass components for production of hydrogen/syngas. *Journal of the Energy Institute*, 92, 1987-1996, 2019.
- [40] Yang, H., Yan R., Chen H., Lee D.H., Zheng C., Characteristics of hemicellulose, cellulose and lignin pyrolysis. *Fuel*, 86, 1781-1788, 2007.
- [41] Williams P.T., Hydrogen and carbon nanotubes from pyrolysis-catalysis of waste plastics: A review. *Waste & Biomass Valorization*, 12(1), 1-28, 2021.
- [42] Bartholomew, C.H. Sintering kinetics of supported metals: new perspectives from a unifying GPLE treatment. *Applied Catalysis A: General*, 107, 1-57, 1993.
- [43] Zhou L., Wang Y., Huang Q., Cai J. Thermogravimetric characteristics and kinetic of plastic and biomass blends co-pyrolysis *Fuel Processing Technology*, 87, 963-969, 2006.
- [44] Li, X., Zhang, H., Li, J., Su, L., Zuo, J., Komarneni, S., Wang, Y. Improving the aromatic production in catalytic fast pyrolysis of cellulose by co-feeding low-density polyethylene. *Appl. Catal. A: Gen.* 455, 114–121, 2013.
- [45] Gunasee S.D., Danon B., Gorgens J.F., Mohee R., Co-pyrolysis of LDPE and cellulose: Synergies during devolatilization and condensation. *Journal of Analytical & Applied Pyrolysis*, 126, 307-314, 2017.
- [46] Oyedun A.O., Tee C.Z., Hanson S., Hui C.W. Thermogravimetric analysis of the pyrolysis characteristics and kinetics of plastics and biomass blends., *Fuel Processing Technology*, 128, 471-481, 2014.
- [47] Ryu H.W., Kim D.H., Jae J., Lam S.S., Park E.D., Park Y.K. Recent advances in catalytic co-pyrolysis of biomass and plastic waste for the production of petroleum-like hydrocarbons. *Bioresource Technology*, 310, #123473, 2020.
- [48] Akubo K., Nahil M.A., Williams P.T. Co-pyrolysis-catalytic steam reforming of cellulose/lignin with polyethylene/polystyrene for production of hydrogen. *Waste Disposal & Sustainable Energy* 2, 177–191, 2020.

Figure Captions

Figure 1. Schematic diagram of the two-stage pyrolysis-catalytic Steam/CO reforming reactor system.

Figure 2(a) - 2(f). DoE Response surface plots (RSP) for H₂ production in relation to varying two factors whilst keep the other two factors at the central point. (a) hydrogen yield; steam:CO₂ ratio; catalytic reforming temperature; (b) hydrogen yield; catalyst:RDF ratio; reforming gas input:RDF ratio; (c) hydrogen yield; catalyst:RDF ratio; catalytic reforming temperature (d) hydrogen yield; reforming gas input:RDF ratio; catalytic reforming temperature; (e) hydrogen yield; steam:CO₂ ratio; catalyst:RDF ratio; (f) Hydrogen yield; steam:CO₂ ratio; reforming gas input:RDF ratio

Figure 3(a) - 3(f). DoE Response surface plots for CO production varying two factors whilst keep the other two factors at the central point. (a) carbon monoxide yield; catalyst:RDF ratio; reforming gas input:RDF ratio; (b) carbon monoxide yield; catalyst:RDF ratio; catalytic reforming temperature; (c) carbon monoxide yield; reforming gas input:RDF ratio; catalytic reforming temperature; (d) carbon monoxide yield; steam:CO₂ ratio; catalyst:RDF ratio; (e) carbon monoxide yield; steam:CO₂ ratio; reforming gas input:RDF ratio; (f) carbon monoxide yield; steam:CO₂ ratio; catalytic reforming temperature.

Figure 4(a) – 4(f). DoE Response surface plots for H₂:CO production varying two factors whilst keep the other two factors at the central point. (a) H₂:CO ratio; catalyst:RDF ratio; reforming gas input:RDF ratio; (b) H₂:CO ratio; catalyst:RDF ratio; catalytic reforming temperature; (c) H₂:CO ratio; reforming gas input:RDF ratio; catalytic reforming temperature; (d) H₂:CO ratio; steam:CO₂ ratio; catalyst:RDF ratio; (e) H₂:CO ratio; steam:CO₂ ratio; reforming gas input:RDF ratio; (f) H₂:CO ratio; steam:CO₂ ratio; catalytic reforming temperature.

Figure 5. Comparison of Modde Design of Experiments predicted H₂:CO Target ratio of 1:1 compared with experimental data from the two-stage, pyrolysis-catalytic dry/steam reforming experiments.

Figure 6. Comparison of Modde Design of Experiments predicted H₂:CO Target ratio of 2:1 compared with experimental data from the two-stage, pyrolysis-catalytic dry/steam reforming experiments.

Figure 7. Catalyst stability tests for the experimental conditions maintained at the H₂:CO target molar ratio of 1:1

Figure 8. Catalyst stability tests for the experimental conditions maintained at the H₂:CO target molar ratio of 2:1

Figure 9. XRD profiles of 9(a) fresh catalyst; 9(b) used catalyst at target H₂:CO ratio of 1:1; 9(c) used catalyst at target H₂:CO ratio of 2:1; 9(d) stability used catalyst at target H₂:CO ratio of 1:1; 9(e) stability used catalyst at target H₂:CO ratio of 2:1. Phases = ◆ Ni and ● Al₂O₃.

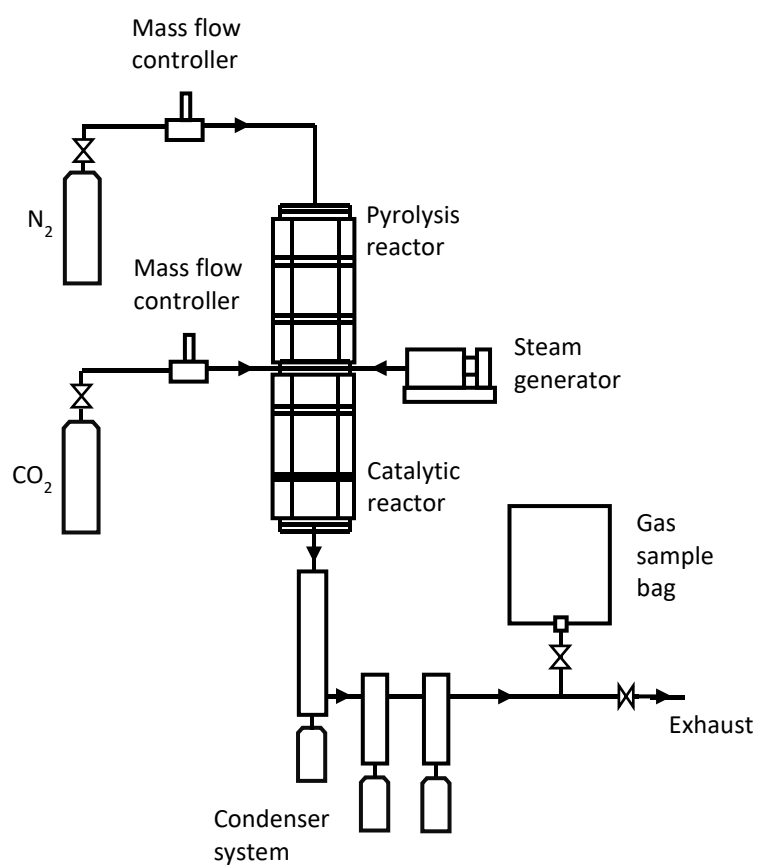


Figure 1. Schematic diagram of the two-stage pyrolysis-catalytic Steam/ CO_2 reforming reactor system.

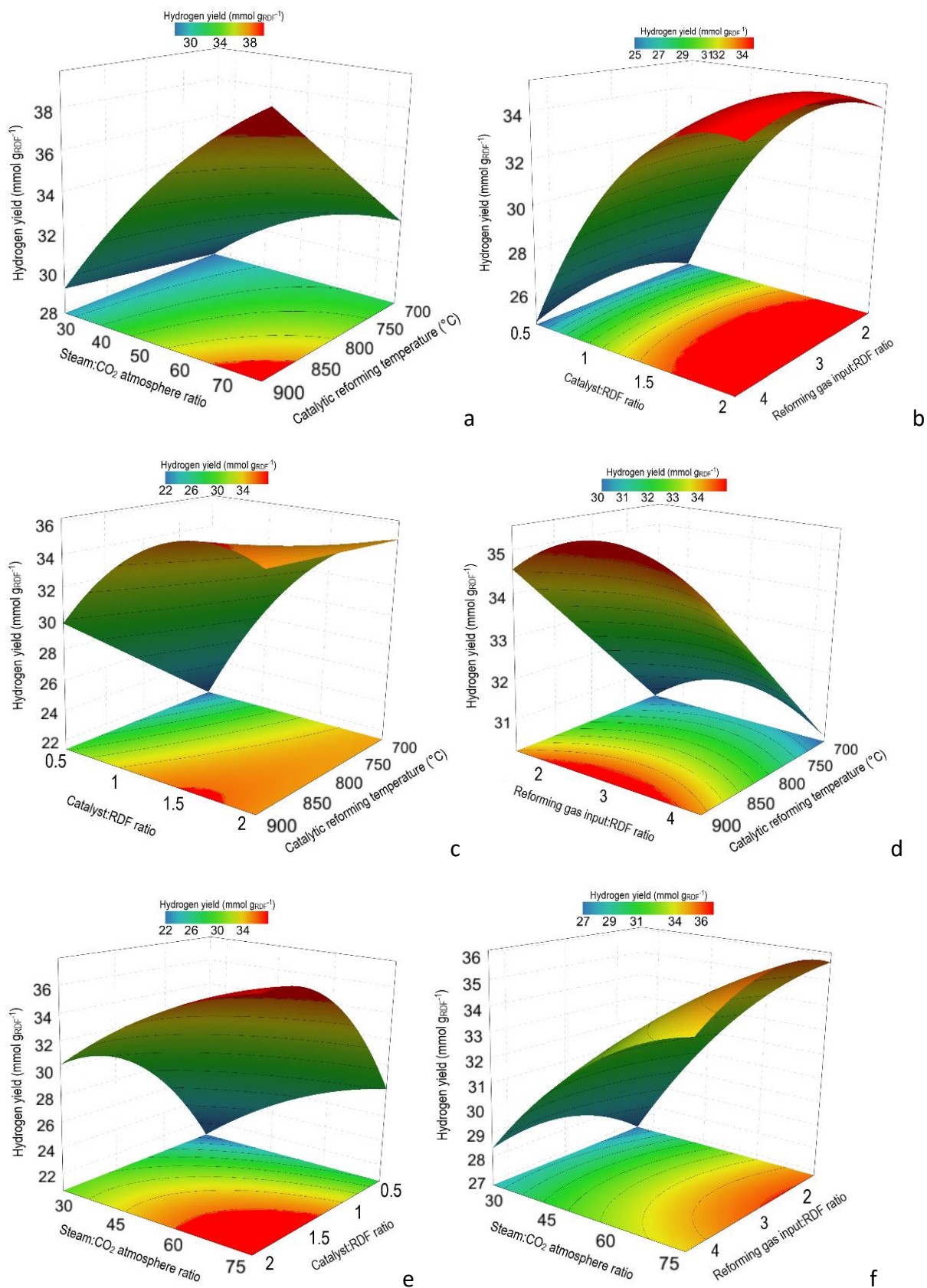


Figure 2(a) - 2(f).

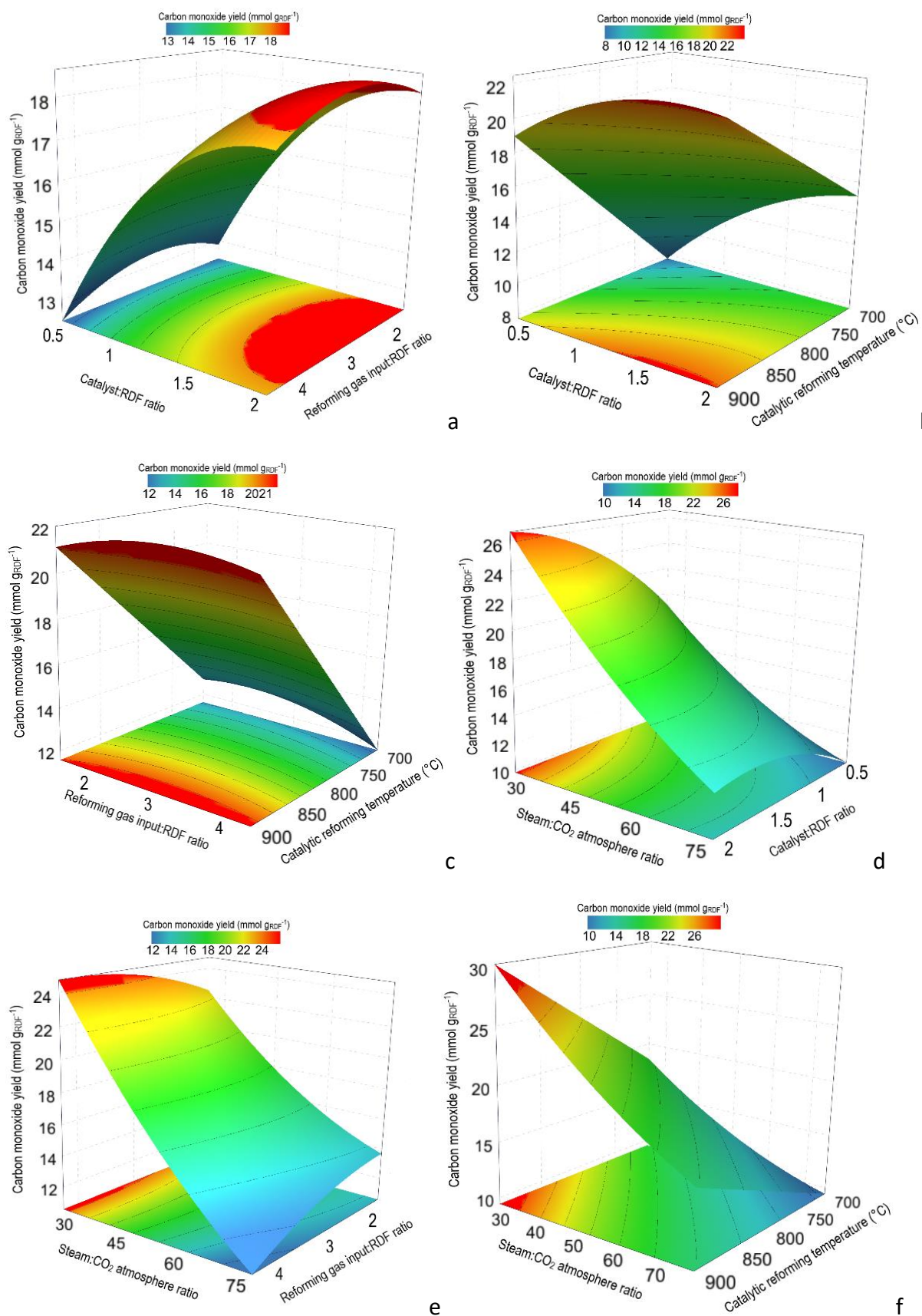


Figure 3(a) - 3(f).

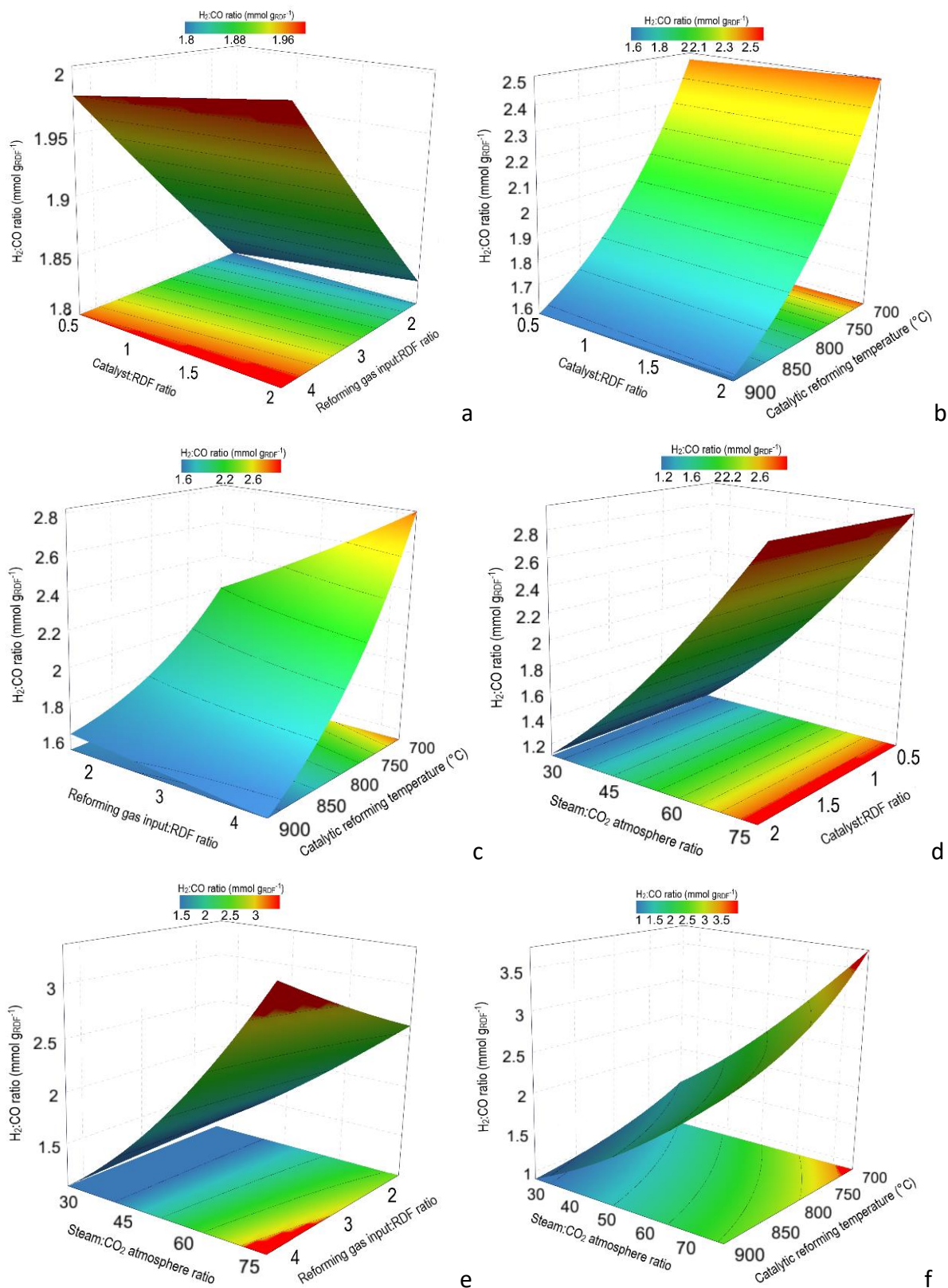


Figure 4(a) – 4(f).

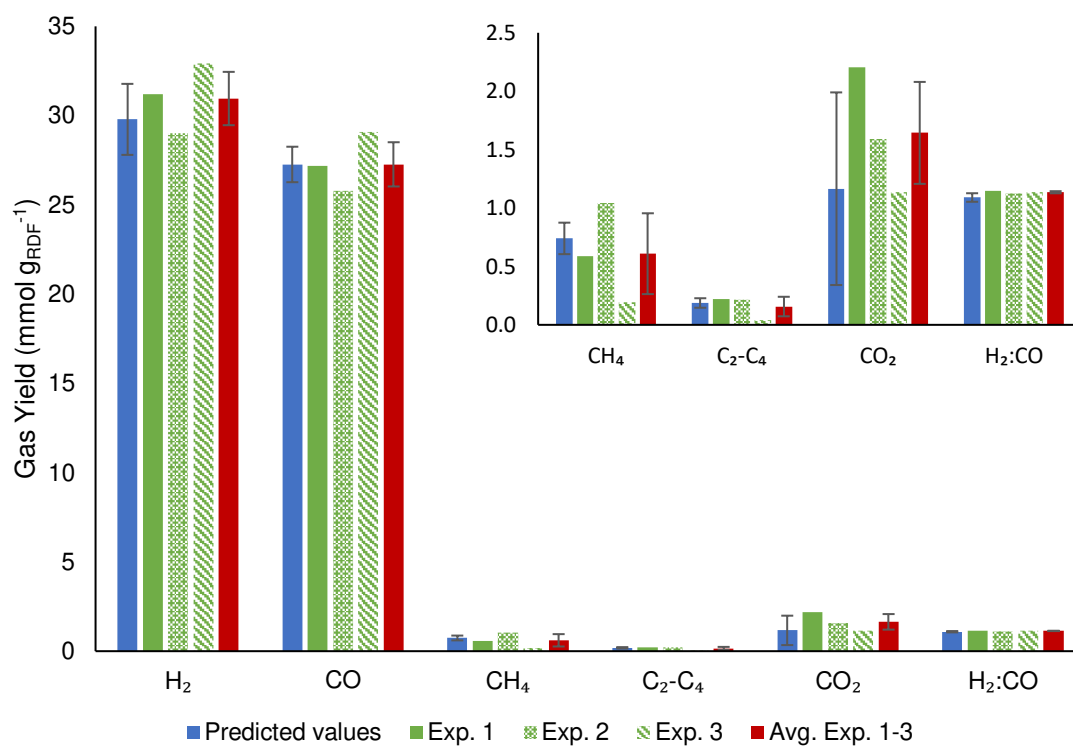


Figure 5. Comparison of Model Design of Experiments predicted H₂:CO Target ratio of 1:1 compared with experimental data from the two-stage, pyrolysis catalytic dry/steam reforming experiments.

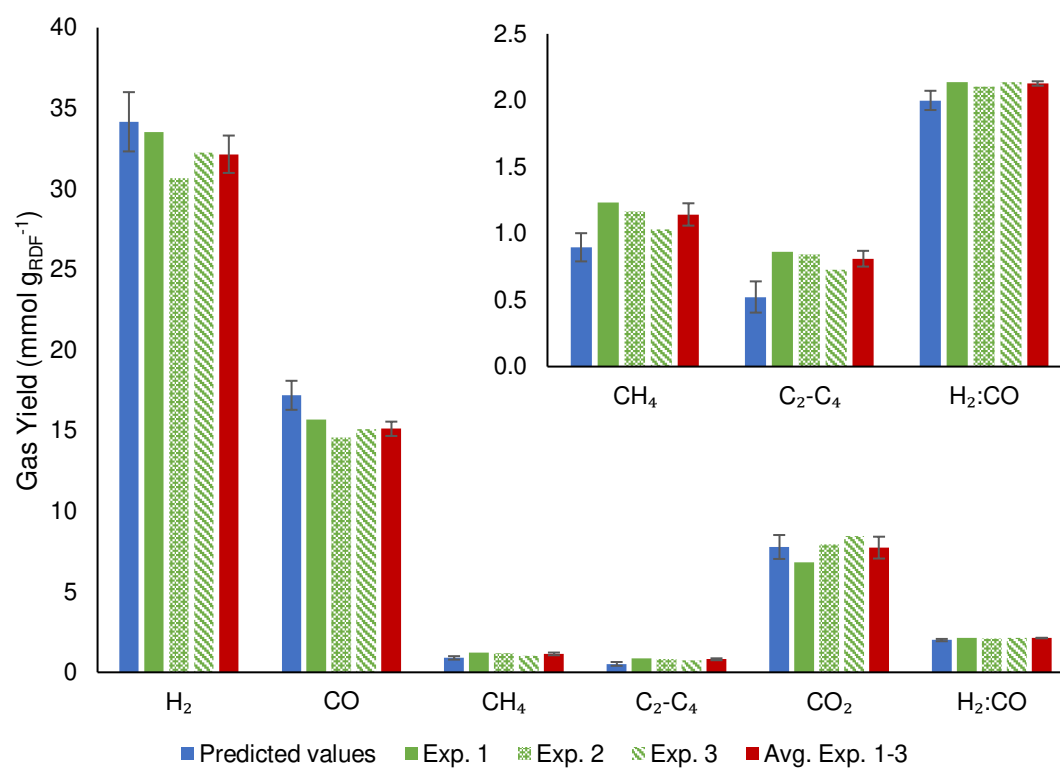


Figure 6. Comparison of Modde Design of Experiments predicted H₂:CO Target ratio of 2:1 compared with experimental data from the two-stage, pyrolysis catalytic dry/steam reforming experiments.

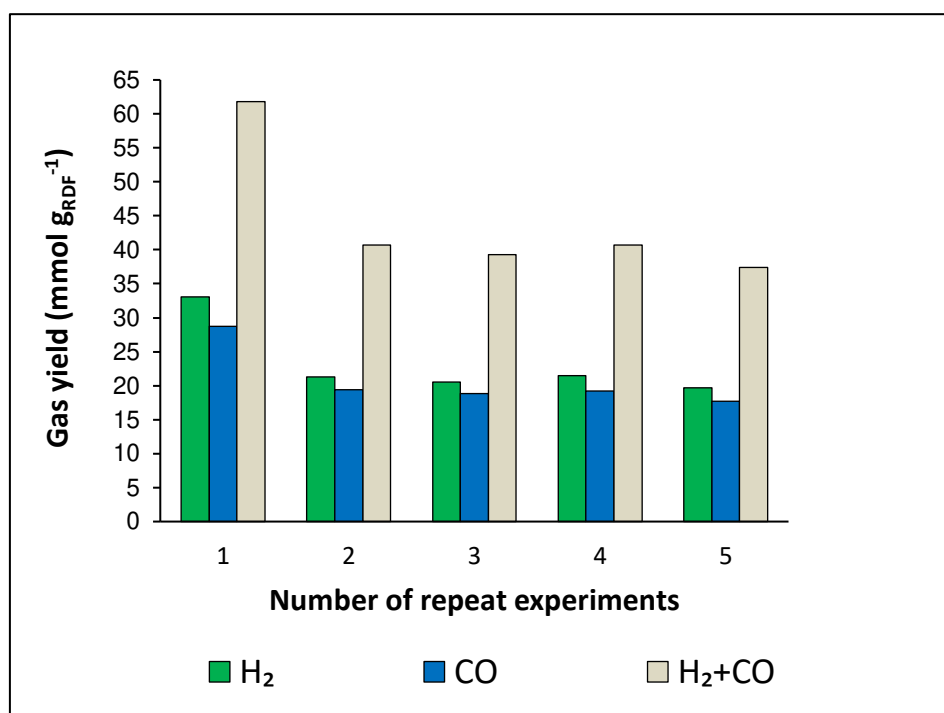


Figure 7. Catalyst stability tests for the experimental conditions maintained at the H₂:CO target molar ratio of 1:1

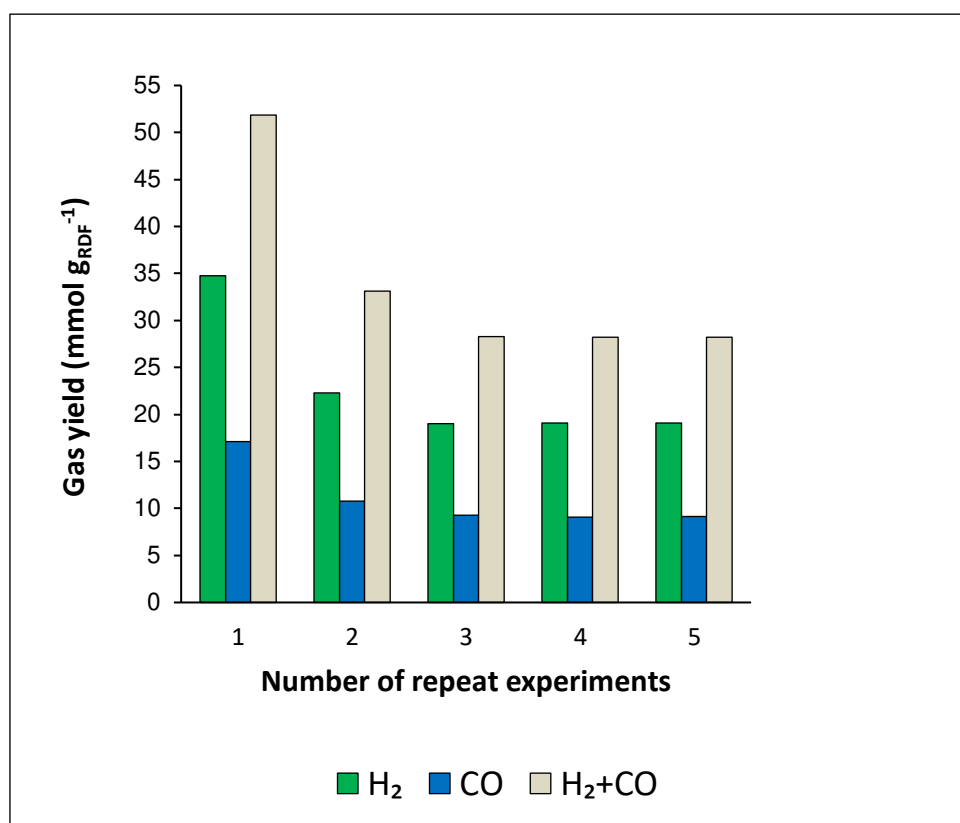


Figure 8. Catalyst stability tests for the experimental conditions maintained at the H₂:CO target molar ratio of 2:1

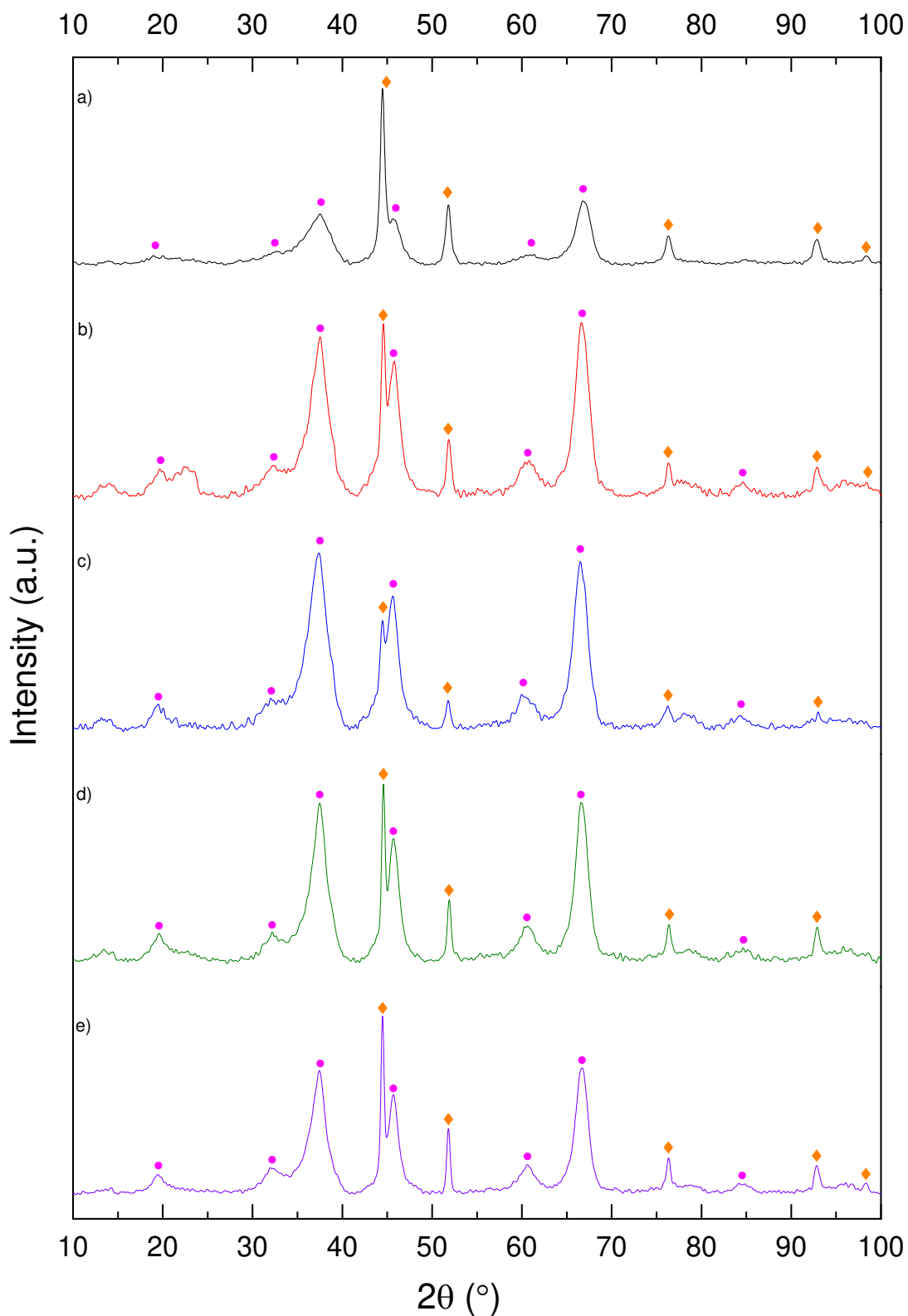


Figure 9. XRD profiles of 9(a) fresh catalyst; 9(b) used catalyst at target $\text{H}_2:\text{CO}$ ratio of 1:1; 9(c) used catalyst at target $\text{H}_2:\text{CO}$ ratio of 2:1; 9(d) stability used catalyst at target $\text{H}_2:\text{CO}$ ratio of 1:1; 9(e) stability used catalyst at target $\text{H}_2:\text{CO}$ ratio of 2:1. Phases = \blacklozenge Ni and \bullet Al_2O_3 .

Table 1. Elemental and proximate analysis of the RDF (as received)

Element analysis (wt.%)		Proximate analysis (wt.%)	
Nitrogen	0.98	Moisture content	3.08
Carbon	43.27	Volatile matter	72.81
Hydrogen	5.30	Fixed carbon	8.12
Sulphur	0.47	Ash	15.99
Oxygen*	30.91		

*by difference

Table 2. Analysis of variance (ANOVA) model data for response variables.

Response	Source	DF	SS	MS	F	P	R₂	R₂ adj.	Q₂
H ₂	Model	10	1107.21	110.72	6.71	<.001	0.807	0.687	0.381
CO	Model	12	1401.53	116.79	31.06	<.001	0.964	0.933	0.848
H ₂ :CO	Model	9	1.194	0.133	111.17	<.001	0.983	0.974	0.954

Table 3. Design of Experiments (DoE) equations 1-3 which show the relationship between the response function and process variables.

Response Function	DoE Equation	Equation number
H ₂	$H_2 = 33.354 + 2.172 X_1 + 0.055 X_2 + 3.744 X_3 + 4.805X_4 - 0.915 X_2^2 - 1.124X_3^2 - 3.024X_4^2 + 1.536X_1X_3 - 1.987X_1X_4 - 0.714X_2X_3$	1
CO	$CO = 17.417 + 4.562 X_1 - 0.217 X_2 - 5.744X_3 + 2.643 X_4 - 0.672 X_2^2 + 1.103 X_3^2 - 1.449 X_4^2 + 0.409 X_1X_2 - 1.218 X_1X_3 - 1.051 X_1X_4 - 1.355 X_2X_3 - 1.120 X_3X_4$	2
H ₂ :CO	$H_2:CO = 0.278 - 0.098 X_1 + 0.021 X_2 + 0.212 X_3 + 0.002 X_4 + 0.020 X_1^2 - 0.020 X_3^2 - 0.033 X_1X_2 + 0.015 X_1X_3 + 0.034 X_2X_3$	3

Table 4. Main process reactions and enthalpy of reaction

Reaction / Process	Equation	ΔH_{298}° KJ mol ⁻¹	
Pyrolysis (biomass)	$C_xH_yO_z \rightarrow H_2 + CO + CO_2 + H_2O + CH_4 + C_nH_m + Tar + Char$		Eq. 1
Pyrolysis (plastics)	$C_xH_y \rightarrow H_2 + CH_4 + C_{x-1}H_{y-1} + Char$		Eq. 2
Steam methane reforming	$CH_4 + H_2O \leftrightarrow CO + 3H_2$	+ 206	Eq. 3
	$CH_4 + 2H_2O \leftrightarrow CO_2 + 4H_2$	+ 165	Eq. 4
Dry methane reforming	$CH_4 + CO_2 \leftrightarrow 2CO + 2H_2$	+ 247	Eq. 5
Hydrocarbon reforming	$C_nH_m + nH_2O \rightarrow nCO + \left(n + \frac{m}{2}\right) H_2$	>0	Eq. 6
	$C_nH_m + nCO_2 \rightarrow 2nCO + \left(\frac{m}{2}\right) H_2$	>0	Eq. 7
Tar reforming	$Tar + H_2O \rightarrow H_2 + CO + CO_2 + C_nH_m$	>0	Eq. 8
Tar cracking	$Tar + Heat \rightarrow H_2 + CO + CO_2 + CH_4 + C_nH_m$	>0	Eq. 9
Water-gas-shift reaction	$CO + H_2O \leftrightarrow CO_2 + H_2$	- 41	Eq. 10
Water gas reaction	$C + H_2O \leftrightarrow CO + H_2$	+ 75	Eq. 11
	$C + 2H_2O \leftrightarrow CO_2 + 2H_2$	+ 119	Eq. 12
Boudouard reaction	$C + CO_2 \leftrightarrow 2CO$	+ 172	Eq. 13

Table 5. Experimental conditions for the target H₂:CO molar ratio of 1:1 and 2:1

Target H₂:CO molar ratio	Catalytic reforming temperature (°C)	Input reforming gas:RDF ratio (g h⁻¹)	Steam:CO₂reforming gas ratio	Catalyst:RDF ratio
1:1 (0.9-1.1:1)	852	3.300:1	27:73	1.325:1
2:1 (1.7-2.2:1)	810	3.585:1	53:47	1.325:1

Table 6. Catalyst properties for the fresh and used catalysts

Catalyst	Surface area (m² g⁻¹)	Pore volume (cm³ g⁻¹)	Pore size (nm)	Catalyst carbon deposits (wt. %)	Ni particle size (nm)³
10 % Ni-Al ₂ O ₃ fresh	134.6	0.394	9.67	-	16.2
Used catalyst target H ₂ :CO ratio 1:1	107.6	0.392	12.40	0.37	18.4
Used catalyst target H ₂ :CO ratio 2:1	109.8	0.393	12.07	0.50	19.5
Used catalyst stability test H ₂ :CO ratio 1:1	85.0	0.387	16.14	n.d.	29.9
Used catalyst stability test H ₂ :CO ratio 2:1	82.5	0.392	16.71	n.d.	32.8